

Microfabricated Chip-Scale Rubidium Plasma Light Source for Miniature Atomic Clocks

Vinu Venkatraman, Yves Pétremand, Christoph Affolderbach, Gaetano Mileti,
Nico F. de Rooij, and Herbert Shea

Abstract—We present the microfabrication and characterization of a low-power, chip-scale Rb plasma light source, designed for optical pumping in miniature atomic clocks. A dielectric barrier discharge (DBD) configuration is used to ignite a Rb plasma in a micro-fabricated Rb vapor cell on which external indium electrodes were deposited. The device is electrically driven at frequencies between 1 and 36 MHz, and emits 140 μW of stable optical power while coupling less than 6 mW of electrical power to the discharge cell. Optical powers of up to 15 and 9 μW are emitted on the Rb D2 and D1 lines, respectively. Continuous operation of the light source for several weeks has been demonstrated, showing its capacity to maintain stable optical excitation of Rb atoms in chip-scale double-resonance atomic clocks.

I. INTRODUCTION

TODAY there exist several varieties of atomic clocks that exploit different atomic transition frequencies, atom/ion containment methods, and interrogation schemes for the realization of highly accurate and stable frequency references. Their frequency instability (Allan deviation) and accuracy generally scale inversely with total clock size. For example, atomic fountain clocks and optical atomic clocks provide the most accurate frequency references (clock uncertainty down to less than 10^{-15}) but occupy volumes of several cubic meters and consume hundreds of watts of power. At the other end of the scale are the compact vapor-cell Rb⁸⁷ double-resonance (DR) microwave frequency standard (overall volumes of 100 to 1000 cm³), that bring the benefits of atomic clocks to applications where mass, volume, and power consumption of the clock are an issue, e.g., in navigation systems [1], network synchronization, and digital communication systems [2]. Even smaller miniature or chip-scale atomic clocks [3] having volumes of a few cubic centimeters and consuming <100 mW of power [4] are now emerging from research to applications, in re-

sponse to an increasing demand for portable or remote operation (e.g., in GNSS receivers).

The compact Rb⁸⁷ DR clocks use light emitted by a Rb discharge lamp for optical pumping and detection of the atomic transitions. These Rb discharge lamps [5] are typically spherical (5 to 10 mm diameter), blown-glass cells filled with a few micrograms of Rb and a few hectopascals of a starter gas for easier ignition of the plasma, which is inductively coupled by an external coil. These lamps operate very well for compact clocks because of the intrinsically correct light frequency for optical pumping (Rb lines), technical simplicity, slow frequency drift (aging), and long lifetime. However, they cannot be used for chip-scale atomic clocks because of their high power consumption (several watts), large size, and non-planar geometry which prevent compact integration (chip-stack configuration, for example) [2]. Hence the DR approach has been a challenge for chip-scale clocks [2] and the coherent population trapping (CPT) approach was widely chosen [2], [6], in which a vertical cavity surface emitting laser diode (VCSEL) is used to create a coherent dark state in the atomic sample. The only study published on the realization of a chip-scale DR clock also employs a VCSEL [7].

Although VCSELs offer several advantages including compact size (\sim cubic millimeters), planar substrates, easy integration with other microfabricated components, and low power consumption (a few milliwatts), they require critical temperature control, sophisticated control electronics for laser frequency stabilization, and complicated set-up procedures [2]. A microfabricated planar low-power Rb plasma discharge light source avoids some of these drawbacks and extends the inherent advantages of Rb discharges, and hence the DR technique, to chip-scale atomic clocks.

Microfabrication of hermetically sealed Rb cells with volumes on the order of 1 cubic millimeter has been a challenge, principally because of the highly reactive nature of Rb. Several groups have reported successful bonding techniques compatible with Rb filling, for instance anodic bonding [7]–[9], soldering [10], [11], and glass-frit bonding [12]. Such cells have been used as reference cells in miniaturized atomic clocks, but not as light sources—in part because of the additional complexity of igniting a stable plasma. Although first studies on micro-cell plasma light sources reported on low-power rare-gas discharges, no Rb light was reported [13]–[15]. Here we present the design, fabrication, and characterization of a planar low-power microfabricated Rb plasma light source emitting on the Rb D1 and D2 lines.

V. Venkatraman and H. Shea are with the Microsystems for Space Technologies Laboratory (LMTS), Ecole Polytechnique Fédérale de Lausanne (EPFL), Neuchâtel, Switzerland (e-mail: vinu.venkat@epfl.ch).

Y. Pétremand and N. F. de Rooij are with Sensors, Actuators, and Microsystems Laboratory (SAMLAB), Ecole Polytechnique Fédérale de Lausanne (EPFL), Neuchâtel, Switzerland.

C. Affolderbach and G. Mileti are with Laboratoire Temps-Fréquence (LTF), University of Neuchâtel, Neuchâtel, Switzerland.

DOI: <http://dx.doi.org/10.1109/TUFFC.2012.2214>

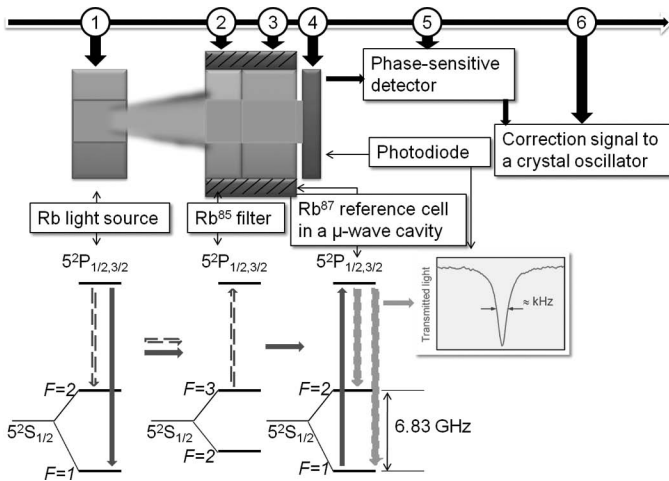


Fig. 1. Operating principle of a DR atomic clock. In the lower part, the level scheme of Rb^{87} is sketched, along with the light emitted (downward arrows) or absorbed (upward arrows) in the respective cells.

II. WORKING PRINCIPLES

A. Double Resonance Rb Atomic Clock

The fundamental concept behind atomic clocks is to exploit an atomic resonance as a reference to stabilize the frequency of a quartz oscillator. In a DR Rb atomic clock [1], this resonance is the clock transition between the two ground-state hyperfine levels of Rb^{87} , at a microwave frequency near 6.83 GHz ($5^2\text{S}_{1/2}$ state, $|F=2, mF=0\rangle$ to $|F=1, mF=0\rangle$), detected on atoms maintained in a small Rb reference cell, as shown in Fig. 1. In a DR Rb clock, pump light from a lamp or laser resonant with the Rb D1 or D2 line (795.0 or 780.2 nm, respectively) illuminates the cell and creates a ground-state polarization in the atoms. The clock transition is then detected by applying a microwave field to the atoms via a microwave-cavity placed around the cell, and the resonance manifests itself as a narrow dip in pump-light power transmitted through the cell versus microwave frequency. The frequency of a voltage-controlled quartz oscillator is locked to this dip using phase-sensitive detection.

Our envisioned DR Rb atomic clock is shown in Fig. 2 and consists of a microfabricated Rb plasma light source, a micro-fabricated Rb^{85} filter, a micro-fabricated Rb reference cell which is enclosed by a miniaturized microwave cavity, and a photodetector. The Rb plasma light source intrinsically emits at the correct wavelengths, Rb D1 and D2 lines, required for a Rb clock.

B. Rb Plasma Light Source

When, after excitation, Rb atoms decay from the $5^2\text{P}_{1/2,3/2}$ states back to the ground state $5^2\text{S}_{1/2}$, they radiate the Rb D1 and D2 wavelengths used for optical pumping of Rb^{87} atoms in Rb atomic clocks. The excitation can be provided by maintaining a sufficiently strong ac electric field across a volume of Rb and buffer gas, where inelas-

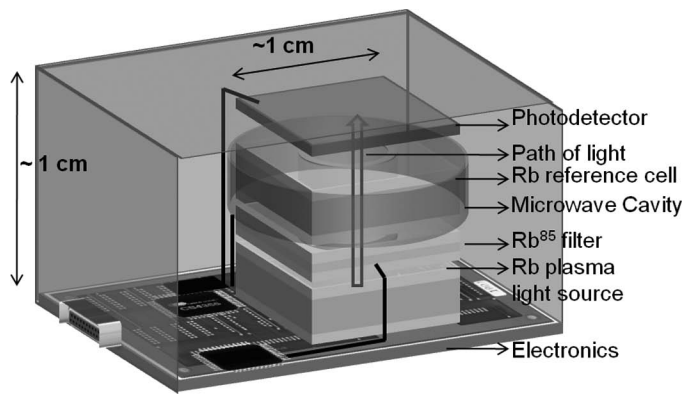


Fig. 2. Schematic representation of the envisioned chip-scale DR clock showing a possible chip-stack configuration.

tic collisions between accelerated electrons and Rb or gas atoms result in excitation and impact ionization [16]. The following de-excitations give rise to a plasma glow discharge [16] and additional electron-ion pairs created by ionizing collisions to an avalanche process and a sustained glow discharge [17].

Designing Rb glow discharge lamps for microfabricated clocks involves four important considerations: low power consumption ($<$ a few milliwatts), small size (a few cubic millimeters), a microfabricated planar structure, and long lifetime (several years). Conventional inductively coupled spherical lamps with diameters of order 1 cm use one or two external RF coils operated at frequencies typically between 75 and 300 MHz consuming several watts of electrical power (80% for light and 20% as heat) to emit electromagnetic discharges (H-discharges) [18] driven by the changing magnetic flux of the coil [19]. Although they are a good choice for compact clocks, they become highly inefficient when miniaturized to chip-scale planar lamps in terms of power requirements (tens of watts) and integration because of the external coil requirements. In principle, a planar spiral coil can be deposited and patterned to inductively couple the plasma [20], but several hundred milliwatts of power will still be required for operation. DC glow discharges, although straightforward, with relatively simple design requirements for chip-scale clocks, need electrodes inside the lamp, allowing electrode erosion during operation and, hence, a shortened lifetime [15], [21]. Other coupling techniques for discharge lamps, namely, the microwave [22] and the traveling wave discharges [16] also require high power (from a few watts to several hundreds of kilowatts) and are expensive, with very low efficiency when scaled down to chip-scale sizes [16].

Dielectric barrier discharges (DBD) are widely used in plasma display panels and other industrial applications. They are based on the same physics as capacitively coupled plasmas (CCP), for which an ac field is used to drive a discharge between metal electrodes [23], but are characterized by the presence of one or more insulating layers in the current path or the discharge gap between the electrodes. DBDs are an efficient low-power technique to

ignite microdischarges across discharge gaps on the order of a millimeter and are therefore chosen for developing the Rb light source reported here.

The two basic configurations that compose DBDs are 1) volume discharges, microdischarges that take place in thin channels between parallel electrodes; and 2) surface discharges, which are usually independent of discharge gap and homogenous over short distances, that take place in thin layers off the dielectric surface [16]. Siliprandi [24] reports that, depending on the buffer gas and pressure in the discharge gap, DBDs operate in two regimes: at low pressure (generally less than 50 hPa), they operate in the Townsend breakdown regime, generating a diffuse glow discharge, whereas at higher pressures (approximately more than 50 hPa), the discharge generally splits up into a large number of randomly distributed microdischarges or current filaments of nanosecond duration also called the streamer regime [24], [25]. In both regimes, the dielectric barrier serves two functions: 1) it distributes the microdischarges evenly over the entire electrode area and 2) it limits the amount of charge and energy that can be fed into an individual microdischarge. After typically a few nanoseconds, the microdischarge is choked because of charge build up on the dielectric, which results in a local reduction of the electric field within the filament [23]. Typically an electric field of few hundred volts per meter is required to sustain a visible glow discharge in these conditions; however, the breakdown voltage required to ignite the discharge is around several hundred volts depending on gas pressure and discharge gap conditions.

We finally note that the mean energy of the electrons and the short duration of the microdischarges strongly limit any heating of the gas atoms, allowing the major fraction of the energy gained by the electrons in the electric field to be deposited in excited atomic states [25].

III. DEVICE MICROFABRICATION

A. Design and Microfabrication

The most important design parameters required to develop the Rb cell for the Rb light source are the discharge gap dimensions, the buffer gas pressure conditions, Rb dispensing, cell substrates, and electrodes. To develop a simple microfabrication process flow for this device, intended for integration with the envisioned chip-stack clock configuration, silicon (relative electrical permittivity 11.68) was chosen as the cell-wall substrate. Transparent Pyrex (Corning Inc., Corning, NY) was chosen for the cell lids on both sides because: 1) it can be anodically bonded with Si to create a hermetic seal, and 2) it is inert with Rb. The chip's lateral dimensions are chosen to be 1×1 cm to integrate with the other 1×1 cm components to form a uniform chip-stack.

Rb vapor density is very low at room temperature ($\sim 10^{-6}$ hPa of vapor pressure at 30°C), and can be increased by increasing the cell temperature (e.g., to

$\sim 10^{-3}$ hPa at 120°C), but one would still require an extremely high electric field to ionize the Rb atoms (Paschen curve) [26] in a pure Rb cell. It is known that plasma displays using DBDs usually work in the pressure-discharge gap (pd) product of 1 to 25 Pa·m range [27] with a preference for higher pressure (p) by adjusting distance (d) for better photon yield (for example NEC uses 670 hPa Xe-Ne and a gap of 100 to 300 μm [28]). A pure Rb cell would thus require a discharge gap of a few meters for a high-yield plasma, and thus a starter gas must be added to achieve a miniature device. Even though higher buffer gas pressure would increase overall photon yield, it will reduce the ratio of Rb spectral lines to that of the buffer gas for a given input power, thus lowering the yield for the Rb light. Hence, following these guidelines and the working regimes of DBDs, a configuration with two different Rb cells with 70 hPa Ar and 30 hPa Ar and a discharge gap of 2 mm was chosen (2-mm-thick Si cell wall with 500- μm -thick Pyrex cell lids). The (pd) products of the cells are 14 and 6 Pa·m, both well within the range of good starting parameters for this device. Argon was chosen because it is inert to Rb, has a relatively smaller diameter, and higher mean free path among noble gases, with an ionization potential of 15.75 eV [17].

The micro-fabricated Rb cell (height: 0.3 cm), consists of a stack of three layers: Pyrex (500 μm thick), silicon (2 mm thick), Pyrex (500 μm thick) which enclose a 5-mm-diameter, 2-mm-thick cylindrical cavity in which a few micrograms of rubidium and the desired pressure of argon are hermetically sealed by a two-step anodic bonding process (Fig. 3). First, the cavity is created by deep reactive-ion etching (DRIE) a through-hole in the silicon wafer. Then, the etched silicon wafer is anodically bonded to the bottom Pyrex layer at 300°C while applying 1000 V between the two layers. After this first bonding step, the natural Rb is dispensed into the cavity under vacuum from a commercial Rb source. The desired pressure of argon is introduced in the chamber, and the top Pyrex layer is anodically bonded to the bottom layers at 300°C and 400 V (for approximately one hour) to create the hermetically sealed Rb vapor cell [29]. A similar process flow was carried out for the Rb^+ 30-hPa cell as well. These two cells will be referred to as the 70-hPa and 30-hPa cells in this paper.

A 200- μm -thick, 4.5-mm inner diameter, and 5.5-mm outer diameter 100% indium solder ring or film is deposited on top of both sides of the Pyrex layers (i.e., outside the cell) to act as capacitive parallel electrodes to couple RF power to the cell. Indium wets glass well and is, hence, a good choice for electrode deposition on the Pyrex walls. The indium (100%) electrodes are deposited by placing and aligning pre-formed indium rings on top of Pyrex layers above the cavity and reflowing using a soldering iron. These external electrodes avoid electrode corrosion and might allow for lower power consumption when compared with the more traditional internal electrode designs [19]. Note that in a future wafer-level production of the plasma light source, the electrodes can be directly integrated

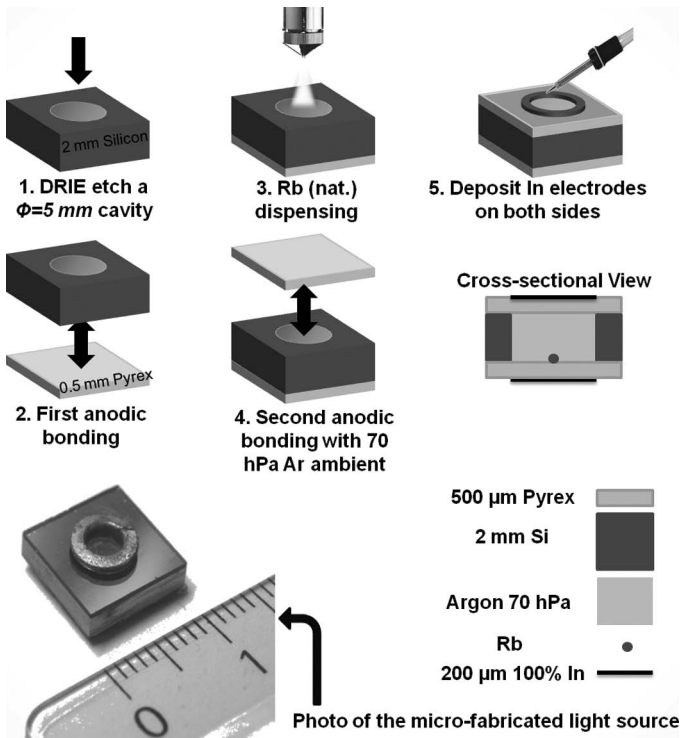


Fig. 3. Microfabrication process flow of the Rb light source showing Rb dispensing and hermetic sealing for the 70-hPa cell. Steps 1 and 2 are performed at wafer level and steps 3 to 5 are completed at chip level. For the 30-hPa cell, the same process flow is used except for the change in Ar pressure.

onto the Pyrex layers by evaporation or sputtering and micropatterning techniques, and could be made of a different metal or transparent metal oxide like ITO to better withstand high temperatures. Our micro-discharge cell design is thus compatible with wafer-level manufacturing of many devices at a time, potentially allowing for greatly reduced cost per unit.

B. RF Drive Electronics Circuit

When DBDs are ignited in an ac field, high-voltage, low-frequency (<500 kHz) operation tends to spread the microdischarges, whereas low-voltage, high-frequency (>500 kHz) operation tends to reignite the same microdischarge channels every half-period [23]. For a given electric field strength, the higher the frequency is, the less kinetic energy the electrons can accumulate during each RF cycle [25], and thus a higher peak voltage is required for plasma ignition at higher frequencies, which can lead to lower power efficiency. In this work, we observed that it was only possible to ignite and sustain a glow discharge within the frequency range of 1 to 36 MHz, with our equipment having a maximum RF power of 10 W, despite adapting the impedance matching circuit for each frequency (see the subsequent discussion).

The microfabricated Rb vapor cell—with the patterned In electrodes—has a measured capacitance of ~ 0.4 pF at frequencies below 10 MHz and up to ~ 1.6 pF at higher

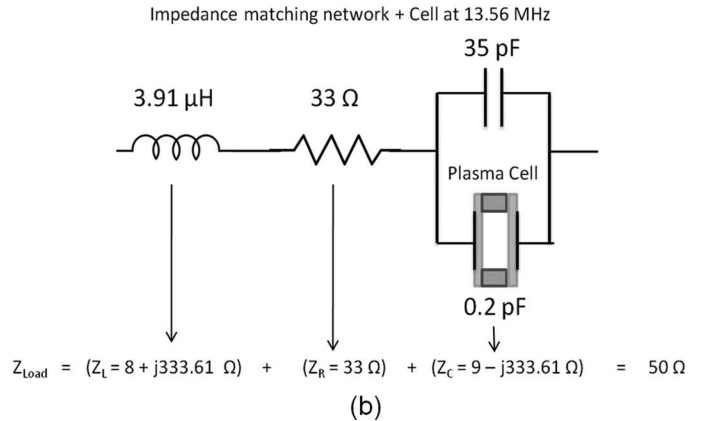
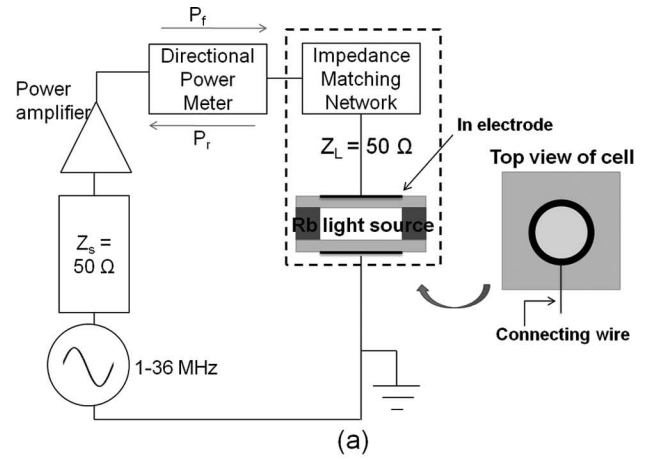


Fig. 4. (a) Schematic of the RF circuitry designed for plasma ignition. (b) An example impedance matching network of LCR components for 13.56 MHz.

frequencies (<36 MHz), and a reactance of $\sim j85$ k Ω at low frequencies (a few megahertz). In our setup, we use a standard laboratory RF generator (33220A, Agilent technologies Inc., Santa Clara, CA; maximum amplitude: 10 V_{pp}) with an output impedance of 50 Ω as the signal source, see Fig. 4(a). To transfer power efficiently to the chip, and to reach the high ac voltage required for breakdown, an impedance matching circuit is thus required. Several circuits based on L-C components were used, an example network is shown in Fig. 4(b). The two main components in the impedance matching network are 1) a capacitor in parallel to the cell to reduce the overall capacitive reactance, and 2) an inductor in series with these capacitors to cancel out the reactive load so as to form a purely resistive load. The values and the equivalent series resistance (ESR) of the components are carefully chosen to maximize the power transfer to the cell.

Because the Rb chip has a very low capacitance, simple parasitic capacitances become non-negligible for impedance matching purposes in the megahertz range. Impedance matching was done with the aid of Smith charts and a network analyzer, but was made efficient by careful measurements of these parasitic capacitances and including a variable capacitor in parallel for tuning. Fig. 5(a) shows the SPICE simulation of the voltage amplification

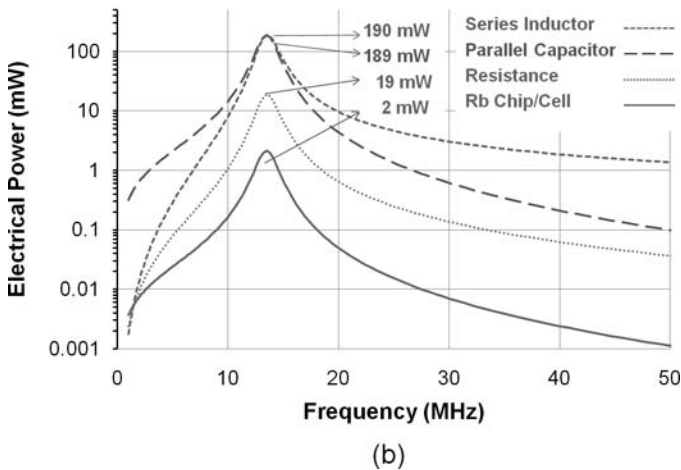
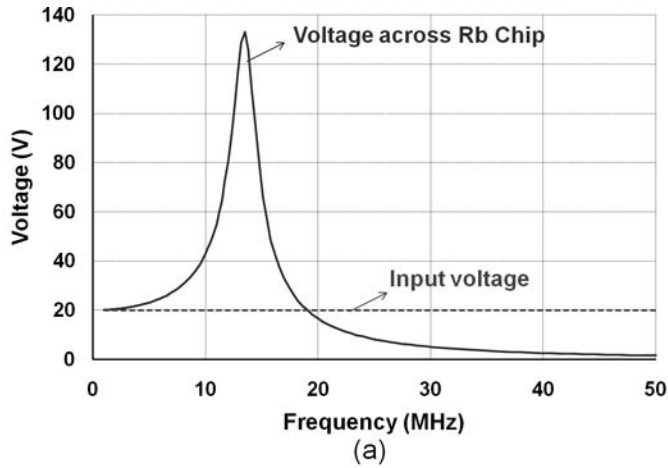


Fig. 5. (a) Greater than $6\times$ voltage amplification is achieved across the Rb chip for the example circuit shown in Fig. 4(b). (b) Power consumption of the different electrical components of the circuit showing $<1\%$ of the total power consumed by the Rb chip.

achieved across the chip at a desired frequency for the example circuit shown in Fig. 4(b). Fig. 5(b) shows the simulation of power consumed by different circuit components for a given input signal for the same circuit. It can be seen that nearly 94% of the power is consumed by the series inductor and parallel capacitor, about 5% is consumed by the series resistance, and $<1\%$ of the total power is coupled to the chip.

IV. RESULTS AND DISCUSSION

The light source using both the 70-hPa and 30-hPa cells were impedance matched, ignited (Fig. 6), and tested at several drive frequencies over the 1 to 36 MHz frequency range. The temperature of the Rb cell was controlled by a small hotplate thermostat placed under the cell. The results reported in this article (a subset of which were also reported in conference proceedings [30], [31]) were obtained at 4.6 MHz, where optimal performance of the device was observed.

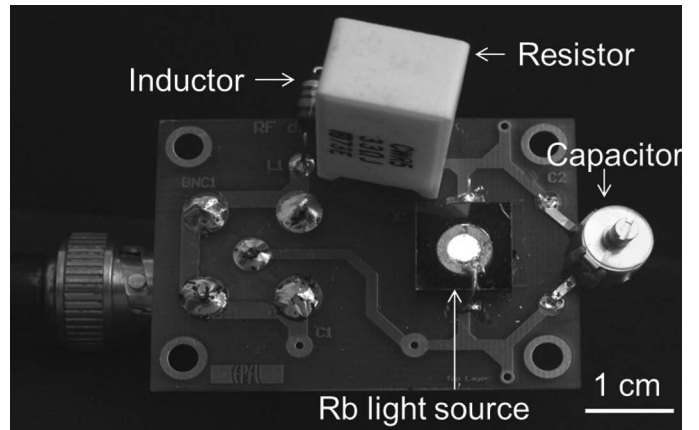


Fig. 6. Photograph of the Rb cell on a printed circuit board connected to *LCR* components emitting the Rb glow discharge when supplied with RF power through a 50- Ω coaxial connection.

A. Output Optical Characteristics

The output optical spectrum of the 70-hPa-cell light source and 30-hPa-cell light source were measured using an Ocean Optics USB4000 spectrometer (Ocean Optics Inc., Dunedin, FL) and are shown in Fig. 7(a) and 7(b) respectively. At room temperature, both Ar and Rb lines are visible with comparable intensity. As the cell temperature is increased, the Rb vapor pressure rises rapidly (by a factor of 100 between 35°C and 90°C), and indeed a strong increase in the intensity of the Rb D1 lines (795.0 nm) and D2 lines (780.2 nm) is observed. This is similar to the behavior observed by [32] and [33] on their comparably sized Rb lamps up to around 120°C. However, the reduction in Rb D line intensity resulting from self-absorption, as observed at temperatures $<120^\circ\text{C}$ in [32] and [33], is not observed in these cells up to 150°C, as expected because of the higher number density of buffer-gas atoms. With increasing cell temperature and increasing emitted Rb light intensity, a reduction of the Ar line intensity is observed. This effect was experimentally observed to be more prominent for the 70-hPa cell [Fig. 8(a)].

The total optical power emitted from the Rb chip was 100 μW when 2 mW of electrical power was coupled to the cell (400 mW are supplied to the impedance matching circuit), as shown in Fig. 8(b). The optical power emitted on the Rb D2 line emitted was 15 μW at a cell temperature of 150°C. This 70-hPa-cell light source was found to be operating distinctly in the streamer regime with several volume microdischarges spread over the dielectric surface at low frequencies (1 to 3 MHz) and maintained the same microdischarge channels at higher frequencies (>4 MHz). More volume discharges were observed as thin channels crossing the discharge gap, the number of microdischarges being proportional to the voltage amplitude. At frequencies ≥ 10 MHz, the discharge was found to become more homogenous, suggesting that the pre-ionization electron density is large enough to cause appreciable overlap and coalescence of primary avalanche heads and smoothing of space-charge field gradients. The 30-hPa-cell light source,

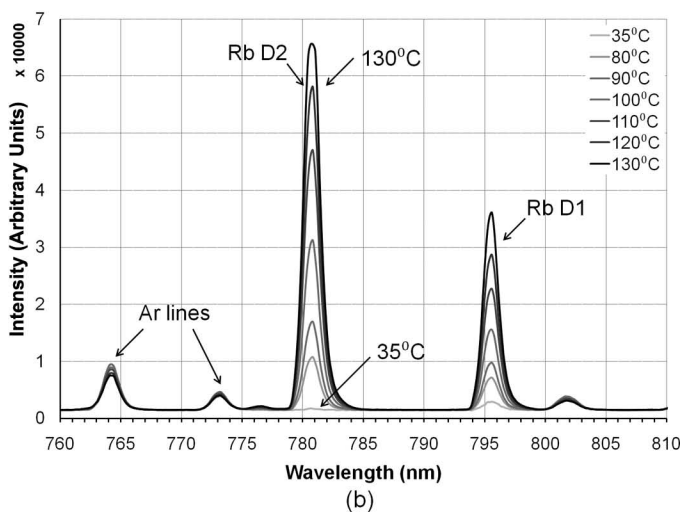
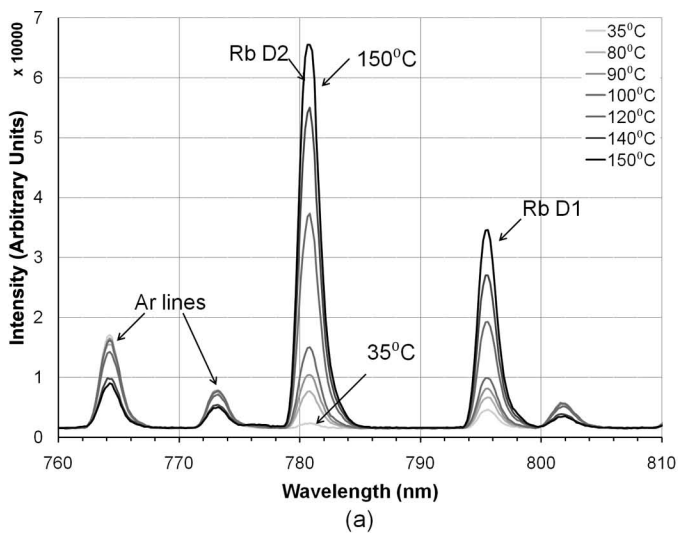


Fig. 7. Output optical spectrum of the (a) 70-hPa cell and (b) 30-hPa cell for temperatures from 25°C to 150°C at 600 mW total input RF power.

on the other hand, was found to operate in the diffuse glow discharge regime (Townsend regime) emitting more of a homogenous surface discharge. Its output spectrum follows the same pattern as for the 70-hPa cell when varying the drive frequency, with an increasing effect of volume discharges at low frequencies (<2 MHz). Because of the nanosecond duration of these DBDs and limited charge transport and energy dissipation, there was very little gas heating: the outside cell temperature was found to be <60°C after several hours of room-temperature operation.

B. Rb Light Power Stability

The optical power of the Rb lines was recorded at a constant RF feed condition for the 70-hPa plasma light source operating at a temperature of 100°C. The short-term (seconds) and long-term (hours) variation in optical power was measured, as shown in Fig. 9.

The average short-term fluctuations in optical intensity of the Rb lines was found to be less than 0.1% and the

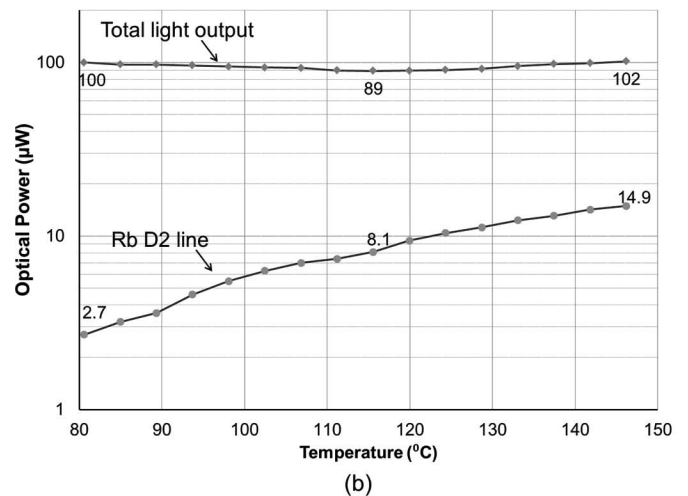
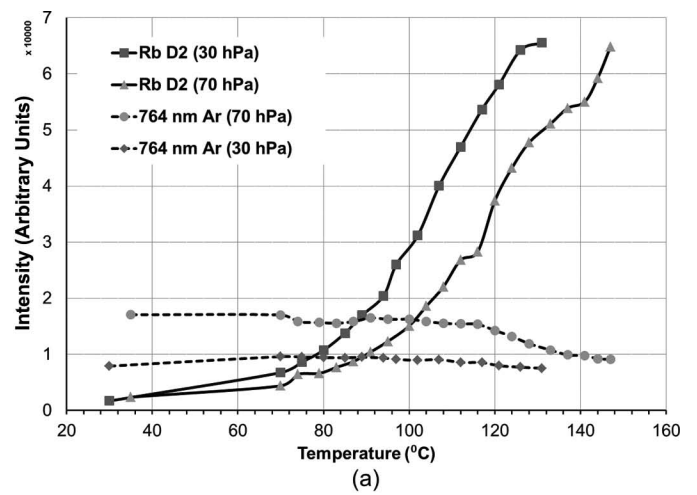


Fig. 8. (a) Comparison of Rb and Ar line intensity variations with temperature in the two cells. (b) Output optical power of the 70-hPa cell as a function of cell temperature.

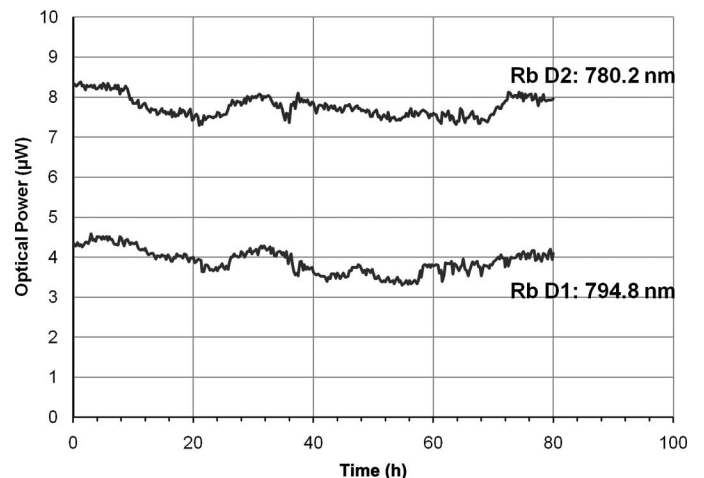


Fig. 9. Rb lines stability with time: 70-hPa cell at 100°C and 600 mW RF input power.

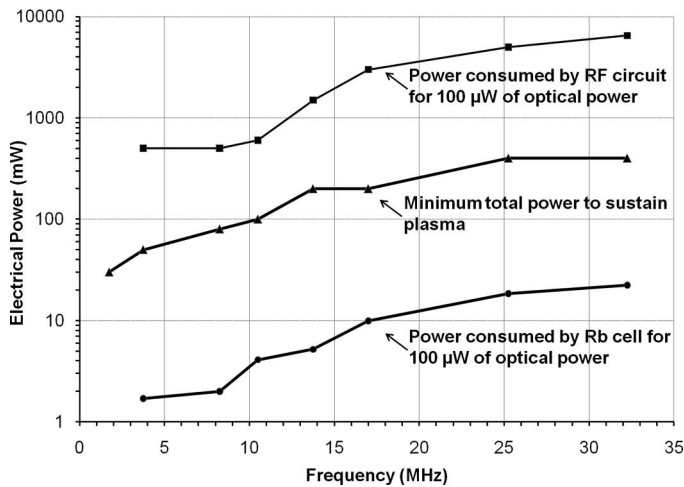


Fig. 10. Electrical power consumption of the cell and circuit versus input ac frequency.

long-term variations were found to be less than 5% (shown in Fig. 9). The primary cause of the long-term variations in optical power is the drift in resistance (2 to 3%) of the electrical components of the impedance matching network with time, mainly resulting from thermal effects. Residual deviations from a perfect correlation between the two curves might well be caused by intensity variations of an Ar emission line close to 795 nm that cannot be separated from the Rb D1 line with the spectrometer used here. These long-term variations can, in principle, be limited to less than 0.01% using a proportional-integral-derivative (PID) feedback loop that controls the input electrical power and/or the RF drive frequency to maintain a steady output light power level. The short-term fluctuations were observed to have lower amplitudes at higher frequencies (>8 MHz) and higher amplitudes at low frequencies resulting from the random distribution of the microdischarge channels in the streamer regime, in which the same microdischarge channels are not reignited during all half cycles [23], [24]. The 30-hPa cell was found to have much less fluctuation of the Rb light power and to emit a constant light power over most of the frequency range, because of the more diffuse glow discharge operation mode.

The plasmas in both cells were ignited several hundred times, and the 70-hPa cell was operated continuously for more than 3 weeks at 100°C, with no degradation. The anodic bonding technique is very robust, and the hermetic seal does not seem to be affected at all by the plasma operation, even at high temperatures.

C. Electrical Power Consumption

As shown in Fig. 10 and in agreement with the arguments of Section III-B, the power required to ignite and sustain a glow discharge increases as the drive frequency increases. This is in agreement with the fact that at low frequencies one achieves higher voltage amplification across the cell because of capacitive coupling. It also partially follows the trend observed by [34], in which the

breakdown voltage is seen to increase with a similar slope with increase in frequency. However, the initial rapid reduction in breakdown voltage observed at low frequencies (1 to 10 MHz in [34]) attributed to the decreasing contribution of drift-dominated electron wall losses [34], is not observed for our plasma lamps down to 1.6 MHz, below which a plasma has not been successfully ignited thus far.

At low frequencies, the power consumed by the cell to emit 100 μ W of power is a few milliwatts, whereas the power consumed by the circuit is more than 100 mW. Hence, the current circuit is not very efficient, with only few percent of the total power being coupled to the cell during operation. Although efficiency is recognized as a challenge for CCPs [16], there is room for improvement in our impedance matching circuit.

V. CONCLUSIONS

A low-power and stable chip-scale Rb plasma light source based on dielectric barrier discharge has been demonstrated, with good potential for wafer-scale fabrication. The light source emits several milliwatts of optical power at the 780.2- and 795.0-nm Rb lines from a 0.3-cm³ chip stack using <6 mW of RF power coupled to the cell (at 1 to 10 MHz). A successful Rb hermetic sealing technique through standard microfabrication processes has been demonstrated. No degradation of the hermetic seal was seen even after several weeks of continuous operation and hundreds of ignitions. The external electrode design implemented eliminates electrode erosion by the plasma, which is the primary lifetime-limiting factor for electrode lamps. The presented plasma light source can be used for hyperfine optical pumping of Rb in novel realizations of atomic devices, such as miniature atomic magnetometers, or when combined with a microfabricated Rb⁸⁵ filter cell [14] in miniature atomic clocks.

ACKNOWLEDGMENTS

We thank our group members for their support and help.

REFERENCES

- [1] F. Droz, P. Rochat, G. Barmaverain, M. Brunet, J. Delporte, J.-F. Dutrey, F. Emma, T. Pike, and U. Schmidt, "On-board Galileo RAFS, current status and performances," in *Proc. 2003 IEEE Int. Frequency Control Symp. jointly with the European Frequency and Time Forum*, 2003, pp. 105–108.
- [2] J. Camparo, "The rubidium atomic clock and basic research," *Phys. Today*, vol. 60, no. 11, pp. 33–39, 2007.
- [3] S. Knappe, "MEMS atomic clocks," in *Comprehensive Microsystems*, vol. 3, Amsterdam, The Netherlands: Elsevier, 2007, pp. 571–612.
- [4] R. Lutwak, "The chip-scale atomic clock—Recent developments," in *Proc. 2009 IEEE Int. Frequency Control Symp. jointly with the European Frequency and Time Forum*, 2009, pp. 573 – 577.
- [5] W. E. Bell, A. L. Bloom, and J. Lynch, "Alkali metal vapor spectral lamps," *Rev. Sci. Instrum.*, vol. 32, no. 6, pp. 688–692, 1961.

- [6] S. Knappe, V. Shah, P. Schwindt, L. Holberg, J. Kitching, L. Liew, and J. Moreland, "A microfabricated atomic clock," *Appl. Phys. Lett.*, vol. 85, no. 9, pp. 1460–1462, 2004.
- [7] A. M. Braun, T. J. Davis, M. H. Kwakernaak, J. J. Michalchuk, A. Ulmer, W. K. Chan, J. H. Abeles, Z. A. Shellenbarger, Y. Y. Jau, W. Happer, T. McClelland, H. Fruehauf, R. Drap, W. Weidemann, and M. Variakojis, "RF-interrogated end-state chip-scale atomic clock," *Proc. 39th Annu. Precise Time and Time Interval Meeting*, 2007, pp. 233–247.
- [8] L.-A. Liew, S. Knappe, J. Moreland, H. Robinson, L. Hollberg, and J. Kitching, "Microfabricated alkali atom vapor cells," *Appl. Phys. Lett.*, vol. 84, no. 14, pp. 2694–2696, 2004.
- [9] A. Douahi, L. Nieradko, J. C. Beugnot, J. Dziuban, H. Maillote, S. Guerandel, M. Moraja, C. Gorecki, and V. Giordano, "Vapour microcell for chip scale atomic frequency standard," *Electron. Lett.*, vol. 43, no. 5, pp. 279–280, 2007.
- [10] F. Vecchio, V. Venkatraman, H. Shea, T. Maedar, and P. Ryser, "Dispensing and hermetic sealing Rb in a miniature reference cell," *Sens. Actuators A*, vol. 172, no. 1, pp. 330–335, 2011.
- [11] Y. Pétremand, C. Schori, R. Straessle, G. Mileti, N. de Rooij, and P. Thomann, "Low temperature indium-based sealing of microfabricated alkali cells for chip scale atomic clocks," in *Proc. European Frequency and Time Forum*, Noordwijk, The Netherlands, 2010, p. 119.
- [12] K. Tsujimoto, Y. Hirai, K. Sugano, T. Tsuchiya, and O. Tabata, "Sacrificial microchannel sealing by glass-frit reflow for chip scale atomic magnetometer," in *Proc. IEEE 24th Int. Conf. MEMS*, Cancun, Mexico, 2011, pp. 368–371.
- [13] H. Guo and A. Lal, "Self-powered photon source," in *IEEE Proc. 12th Int. Conf. Solid State Sensors, Actuators and Microsystems*, 2003, pp. 1474–1477.
- [14] S. Wang, L. Lin, and H. Guo, "Analysis and design of a micromachined Rb⁸⁵ filter in passive rubidium atomic clock," in *Proc. IEEE Int. Conf. Nano/Micro Engineered and Molecular Systems*, 2009, pp. 911–914.
- [15] P. Carazzetti, P. Renaud, and H. Shea, "Micromachined chip-scale plasma light source," *Sens. Actuators A*, vol. 154, no. 2, pp. 275–280, 2009.
- [16] A. Bogaerts, E. Neyts, R. Gijbels, and J. van der Mullen, "Gas discharge plasmas and their applications," *Spectrochim. Acta B*, vol. 57, pp. 609–658, 2002.
- [17] E. Nasser, *Fundamentals of Gaseous Ionization and Plasma Electronics*. New York, NY: Wiley-Interscience, 1971.
- [18] G. Babat, "Electrodeless discharges and some allied problems," *J. Inst. Electr. Eng. Part III: Radio Commun. Eng.*, vol. 94, no. 27, pp. 27–37, 1947.
- [19] D. O. Wharmby, "Electrodeless lamps for lighting: A review," *Proc. Inst. Electr. Eng.*, vol. 140, pp. 465–473, 1993.
- [20] J. A. Hopwood, "A microfabricated inductively coupled plasma generator," *J. Microelectromech. Syst.*, vol. 9, no. 3, pp. 309–313, 2000.
- [21] R. G. Longwitz, "Study of gas ionization in a glow discharge and development of a micro gas ionizer for gas detection and analysis," Ph. D. thesis, Institute of Microsystems and Microelectronics, Ecole Polytechnique Federale de Lausanne, 2004.
- [22] C. M. Ferreira and M. Moisan, *Microwave Discharges, Fundamentals and Applications* (NATO ASI series, Series B: Physics, vol. 302), New York, NY: Springer-Verlag, 1993.
- [23] U. Kogelschatz, B. Eliasson, and W. Egli, "Dielectric barrier discharges. Principle and applications," *J. Phys. IV*, vol. 7, no. C4, pp. 447–466, 1997.
- [24] R. A. Siliprandi, H. E. Roman, R. Barni, and C. Riccardi, "Characterization of the streamer regime in dielectric barrier discharges," *J. Appl. Phys.*, vol. 104, no. 6, art. no. 063309, 2008.
- [25] B. Gellert and U. Kogelschatz, "Generation of excimer emission in dielectric barrier discharges," *Appl. Phys. B*, vol. 42, no. 1, pp. 14–21, 1991.
- [26] F. Paschen, "Über die zum funkenübergang in luft, wasserstoff und kohlenensäure bei verschiedenen drücken erforderliche potentialdifferenz," *Ann. Phys.*, vol. 37, no. 5, pp. 69–75, 1889. (in German)
- [27] K. C. Choi, G. F. Saville, and S. C. Lee, "Microbridge plasma display panel with high gas pressure," *IEEE Trans. Electron Devices*, vol. 45, no. 6, 1998.
- [28] T. Akiyama, "Evaluation of discharge cell structure for color AC plasma display panels," in *Proc. 15th Int. Display Res. Conf.*, 1995, pp. 377–380.
- [29] J. DiFrancesco, F. Gruet, C. Schori, C. Affolderbach, R. Matthey, G. Mileti, Y. Salvadé, Y. Petremand, and N. De Rooij, "Evaluation of the frequency stability of a VCSEL locked to a micro-fabricated rubidium vapour cell," *Proc. SPIE*, vol. 7720, art. no. 77201T, 2010.
- [30] V. Venkatraman, Y. Petremand, C. Affolderbach, G. Mileti, N. de Rooij, and H. Shea, "Microfabrication and packaging of a rubidium vapor cell as a plasma light source for MEMS atomic clocks," in *Proc. Transducers 2011*, pp. 1907–1910.
- [31] V. Venkatraman, Y. Petremand, C. Affolderbach, G. Mileti, N. de Rooij, and H. Shea, "Low-power chip-scale rubidium plasma light source for miniature atomic clocks," in *Proc. Int. Frequency Control Symp.–European Frequency and Time Forum 2011*, pp. 1–4.
- [32] H. Fukuyo, K. Iga, N. Kuramochi, and H. Tanigawa, "Temperature dependence of hyperfine spectrum of Rb D1 line," *Jpn. J. Appl. Phys.*, vol. 9, no. 7, pp. 729–734, 1970.
- [33] J. C. Camparo and R. Mackay, "Spectral mode changes in an alkali RF discharge," *J. Appl. Phys.*, vol. 101, no. 5, art. no. 053303, 2007.
- [34] J. L. Walsh, Y. T. Zhang, F. Iza, and M. G. Kong, "Atmospheric-pressure gas breakdown from 2 to 100 MHz," *Appl. Phys. Lett.*, vol. 93, no. 23, art. no. 221505, 2008.



Vinu Venkatraman received his B.E. (Honors) degree in electrical and electronics and M.Sc. (Honors) degree in chemistry from the Birla Institute of Technology and Science, Pilani, India, in 2006 and an M.S. degree in electrical engineering from Portland State University, Portland, OR, in 2008.

Since 2009, he has been pursuing his Ph.D. degree at the Microsystems for Space Technologies Laboratory, EPFL, Switzerland.



Yves Pétremand received the Ph.D. degree from the Institute of Microtechnology of the University of Neuchâtel, Switzerland, in 2008.

Since June 2008, he has been working at EPFL, Switzerland, as a scientist. His major research interests include microfabrication technologies for various applications, especially technologies based on silicon bulk micromachining.



Christoph Affolderbach received his Diploma and Ph.D. degrees, both in physics, from Bonn University, Germany, in 1999 and 2002, respectively. From 2001 to 2006, he was a research scientist at the Observatoire Cantonal de Neuchâtel, Neuchâtel, Switzerland. In 2007, he joined the Laboratoire Temps-Fréquence at the University of Neuchâtel, Neuchâtel, Switzerland as scientific collaborator.

His research interests include the development of stabilized diode laser systems, atomic spectroscopy, and vapor-cell atomic frequency standards, in particular laser-pumped high-performance atomic clocks and miniaturized frequency standards.



Gaetano Mileti received his engineering degree in physics from the Swiss Federal Institute of Technology, Lausanne, Switzerland, in 1990 and the Ph.D. degree in physics from the Neuchâtel University, Neuchâtel, Switzerland, in 1995. From 1991 to 1995 and from 1997 to 2006, he was a research scientist at the Observatoire Cantonal de Neuchâtel. From 1995 to 1997, he was a guest scientist at the National Institute of Standards and Technology, Boulder, CO.

In 2007, he co-founded the Laboratoire Temps-Fréquence (LTF) at the University of Neuchâtel, where he is deputy director and head of research. His research interests include atomic spectroscopy, stabilized lasers, and frequency standards.



Nico F. de Rooij received a Ph.D. degree from the Twente University of Technology, The Netherlands, in 1978. From 1978 to 1982, he worked at the Research and Development Department of Cordis Europa N.V., The Netherlands. In 1982, he joined the IMT of the University of Neuchâtel as professor and head of SAMLAB. Since 1987, he has been a lecturer at ETHZ, and since 1989, he has also been a professor at the EPFL.

In 2008, he became vice-president of CSEM SA, where he is in charge of the Microsystems Technology Division. Currently, he is the director of the Institute of Microengineering at EPFL. His research activities include microfabricated sensors, actuators, and microsystems. He is Head of SAMLAB, with more than 30 staff members, 300 referred publications, and several patents. In 2007, he was the recipient of the IEEE Jun-ichi Nishizawa Medal for “pioneering contributions to microsystem technology and effective transfer into industrial products and applications.”



Herbert R. Shea (SM’2009) received a B.Sc. degree (1991) in physics from McGill University, Montreal, Canada, in 1991, and M.A. and Ph.D. degrees in physics from Harvard University, Cambridge, MA, in 1993 and 1997, respectively.

He developed carbon nanotube FETs at IBM’s T. J. Watson Research Center in Yorktown Heights, NY, from 1997 to 1999, then joined Lucent Technologies’ Bell Labs in Murray Hill, NJ, where he became the technical manager of the Microsystems Technology group, specializing in MEMS reliability. In 2004, he founded the Microsystems for Space Technologies Laboratory at the EPFL (Ecole Polytechnique Fédérale de Lausanne) in Switzerland, where he has been an associate professor since 2011. His current research topics include micromachined polymer actuators, electric micro-propulsion for small spacecraft, MEMS sensors for satellites, MEMS reliability, and chip-scale plasma light sources.